A Study on Continuous Max-Flow and Min-Cut Approaches

Jing Yuan
Computer Science Department, University of Western Ontario
Middlesex College 240, University of Western Ontario, London, ON, Canada, N6A 5B7
cn.yuanjing@gmail.com

Egil Bae
Department of Mathematics, University of Bergen
University of Bergen, Johaness Brunsgate 12, Bergen 5007, Norway
Egil.Bae@math.uib.no

Xue-Cheng Tai
Department of Mathematics, University of Bergen
University of Bergen, Johaness Brunsgate 12, Bergen 5007, Norway
tai@math.uib.no

Abstract

We propose and study novel max-flow models in the continuous setting, which directly map the discrete graph-based max-flow problem to its continuous optimization formulation. We show such a continuous max-flow model leads to an equivalent min-cut problem in a natural way, as the corresponding dual model. In this regard, we revisit basic conceptions used in discrete max-flow / min-cut models and give their new explanations from a variational perspective. We also propose corresponding continuous max-flow and min-cut models constrained by priori supervised information and apply them to interactive image segmentation/labeling problems. We prove that the proposed continuous max-flow and min-cut models, with or without supervised constraints, give rise to a series of global binary solutions $\lambda^*(x) \in \{0, 1\}$, which globally solves the original nonconvex image partitioning problems. In addition, we propose novel and reliable multiplier-based max-flow algorithms. Their convergence is guaranteed by classical optimization theories. Experiments on image segmentation, unsupervised and supervised, validate the effectiveness of the discussed continuous max-flow and min-cut models and suggested max-flow based algorithms.

1. Introduction

Max-flow and min-cut is one of the key strategies to model and solve practical problems in image processing and computer vision as energy minimization procedures. It has been successfully applied in a wide class of applications, e.g. image segmentation [7, 2], stereo [15], 3D reconstruction [17]. The associated energy minimization problem is often mapped as a minimum cut problem on an appropriate graph, and then solved by efficient algorithms of max-flow. There were a vast amount of research works on this topic during the last years [6, 7]. One main drawback of such discrete approaches is the grid bias. The pair-wise interaction potential penalizes some spatial directions more than other, which leads to visual artifacts in the final solution. This is often called metrication errors. Reducing such visual effects often amounts to an extra memory and computational burden [13].

During these years, extensive attentions have been paid to investigate max-flow and min-cut models in a continuous framework. G. Strang [19, 20] was the first to study the max-flow / min-cut related optimization problem over a continuous domain. In [2, 3], Appleton *et al*. proposed a continuous minimal surface approach to segmenting 2D and 3D objects and solved it by PDEs. Chan *et al*. [10] proposed the segmentation of a continuous image domain by a convex approach, which relaxed the binary constraint of the partition function $\lambda(x) \in \{0, 1\}$ to the convex set $\lambda(x) \in [0, 1]$:

$$\min_{\lambda(x)\in[0,1]} \int_\Omega (1-\lambda) f_1 \, dx + \int_\Omega \lambda f_2 \, dx + \alpha \mathrm{TV}(\lambda) \,. \quad (1)$$

The authors proved that (1) leads to a series of global binary optimums by simply thresholding the optimum $\lambda^*(x) \in$

978-1-4244-6985-7/10/$26.00 ©2010 IEEE

$[0, 1]$ of (1). It, consequently, leads to a set of global binary optima to the original nonconvex partition problem. In this regard, it can actually be seen as a continuous min-cut model without priori supervision. Recently, Chan's model (1) was extended to more than two regions in [18, 16, 4], which proposes multi-way cuts in a continuous configuration and was applied to solve multi-labeling problems.

However, in view of the duality between graph-based max-flow and min-cut, the concerning max-flow model, which is dual to the concerning min-cut model over a spatially continuous domain, e.g. (1), is still lost in recent developments. On the other hand, the continuous min-cut model is numerically treated as a normal optimization problem, where potential max-flow features are not studied and explored, both theoretically and numerically. This is not the case in discrete settings where max-flow formulations are often employed to design fast algorithms. Moreover, studies of continuous max-flow and min-cut models with priori supervised constraints are also lost. Simply putting large positive values to specified data, as done in graph-based approaches, distorts numerical schemes in continuous optimization and slows down convergence.

1.1. Contributions

In this paper, we propose and study a new continuous max-flow formulation, which is the direct counterpart, in the continuous spatial setting, of the discrete max-flow model. We generalize the main contributions of this work as follows:

First, we build up the novel continuous max-flow model, in terms of a flow representation and show it is dual to the continuous min-cut problem (1). In comparison to previous works, we show how to compute the continuous min-cut by its max-flow formulation.

Second, we revisit and give a new explanation of the fundamental conceptions in graph cuts, e.g. 'saturated' / 'unsaturated' flows and 'cuts', from a variational perspective. We prove that there exist a series of global binary optima to the new continuous min-cut model, by using the maximal flow formulation, and each resulted cut shares the same energy.

Third, we also propose new continuous max-flow and min-cut models for the segmentation under supervised constraints. Through them, it is not required to change any value of data terms as applied in interactive graph-cuts. Meanwhile, the complexities of the new supervised max-flow and min-cut models are the same as the unsupervised ones. We prove that there exist globally optimal supervised 'cuts', which can be resolved from the global non-binary optimum λ^*.

Last but not least, novel multiplier-based max-flow algorithms are proposed, which, in nature, splits the optimization problem into simple subproblems over independent flow variables. The labeling function $\lambda(x)$ works as the multiplier and is resolved simultaneously. The numerical scheme is reliable and can be verified by classical optimization theories.

2. Continuous Max-Flow and Min-Cut

2.1. Revisit of Discrete Max-Flow and Min-Cut

Many imaging and vision tasks can be formualted in terms of max-flow and min-cut on appropriate graphs, starting from the work of Greig et. al. [11]. A graph $G = (V, E)$ consists of a vertex set V and an edge set $E \subset V \times V$. The vertex set of commonly-used graphs in image processing and computer vision includes the nodes in a 2-D or 3-D nested grid, together with two terminal vertices, the source s and the sink t. The edge set includes two types of edges: the spatial edge e_n sticks to the given grid and links two neighbour grid stencils except s and t; the terminal edge or data edge, e_s or e_t, which links the specified terminal, s or t, to each grid node respectively. We assign a cost $C(e)$ to each edge e, which is assumed to be nonnegative i.e. $C(e) \geq 0$. In this work, we consider this type of graphs in the 2-D case mainly for simplicities. Discussions can be simply extended to the 3-D case.

A two-partition cut assigns the two disjoint partitions to the source s and the sink t respectively, which is also called *s-t cut*. It divides the spatial grid nodes of Ω into two disjoint sets: one relates to the source s and the other to the sink t, hence segments the given image domain into two parts:

$$V \,=\, V_s \bigcup V_t \,, \quad V_s \cap V_t \,=\, \emptyset \,.$$

The energy of each cut is the total cost of edges $e \in E_{st} \subset E$, whose end-points belong to two different partitions. The problem of min-cut is to find the two partitions of vertices such that the corresponding cut-energy is minimal:

$$\min_{E_{st} \subset E} \sum_{e \in E_{st}} C(e) \,. \tag{2}$$

On the other hand, each edge $e \in E$ can be viewed as a pipe and the edge cost $C(e)$ can be regarded as the capacity of this pipe. For such a 'pipe' network, we have the following constraints:

- Capacity of spatial flows p: for an undirected grid edge $e_n \in E$, the spatial flow $p(e_n)$ is constrained:

$$|p(e_n)| \,\leq\, C(e_n) \,; \tag{3}$$

- Capacity of source flows p_s: for a source edge $e_s(v) : s \,\rightarrow\, v$ linking s to the node $v \,\in\, V \backslash \{s, t\}$, $p_s(v)$ is directed from s to v. The capacity $C_s(v)$ indicates that

$$0 \,\leq\, p_s(v) \,\leq\, C_s(v) \,; \tag{4}$$

- Capacity of sink flows p_t: for a sink edge $e_t(v) : v \to t$ linking the node $v \in V\backslash\{s,t\}$ to t, $p_t(v)$ is directed from v to t. Its capacity $C_t(v)$ indicates that

$$0 \,\le\, p_t(v) \,\le\, C_t(v)\,; \tag{5}$$

- Flow conservation: at each node $v \in V\backslash\{s,t\}$, incoming flows are balanced by outcoming flows, i.e. all the flows passing v should be constrained by:

$$\big(\sum_{e_n \in N(v)} p(e_n)\big) - p_s(v) + p_t(v) \,=\, 0\,. \tag{6}$$

  where $N(v) \subset E$ is the set of edges linking v to its neighbour nodes.

The maximal flow problem tries to find the largest flow amount allowed from the source s, i.e.

$$\max_{p_s} \sum_{v \in V\backslash\{s,t\}} p_s(v)\,, \tag{7}$$

subject to the above conditions (3), (4), (5) and (6).

When a flow $p(e)$ over the edge $e \in E$ reaches its corresponding capacity $C(e)$, in (3), (4) or (5), we call it 'saturated'; otherwise, 'unsaturated'. It is well known that the max-flow problem (7) is equivalent to the min-cut problem (2), where the flows are saturated uniformly on the cut edges, i.e. flow is bottlenecked by the 'saturated' pipes.

2.2. Primal Model: Continuous Max-Flow

Let Ω be a closed and continuous 2-D or 3-D domain and s, t be the source and sink terminals. At each position $x \in \Omega$, we denote the usual spatial flow passing x by $p(x)$; the directed source flow from s to x by $p_s(x)$; and the directed sink flow from x to t by $p_t(x)$. Now we consider the counterpart of the discrete max-flow problem (7) in this continuous setting, which can be directly formulated in the same manner as stated in the previous section.

In view of the flow constraints (3), (4), (5) and (6) over the graph G, we suggest constraints for flow functions $p(x)$, $p_s(x)$ and $p_t(x)$ over the spatial domain Ω, similarly:

$$|p(x)| \,\le\, C(x)\,; \tag{8}$$

$$p_s(x) \,\le\, C_s(x)\,; \tag{9}$$

$$p_t(x) \,\le\, C_t(x)\,; \tag{10}$$

$$\operatorname{div} p(x) - p_s(x) + p_t(x) \,=\, 0\,, \tag{11}$$

where $C(x)$, $C_s(x)$ and $C_t(x)$ are given capacity functions and $\operatorname{div} p$ evaluates the total incoming spatial flow locally around x, in analogy with the sum operator in (6). The constraints (9) and (10) for the source flow $p_s(x)$ and the sink flow $p_t(x)$ are changed a little in comparison to (4) and (5). This is because the positiveness of flows $p_s(x)$ and $p_t(x)$ are not needed as they are directed flows and their values simply mean that some flows are distributed from s to the pixel x or from x to t. Likewise, $C_s(x)$ and $C_t(x)$ are also not necessary to be positive. This extends the application range of max-flow and min-cut models.

Consider the discrete max-flow problem (7), the *continuous max-flow* model can then be formulated as

$$\max_{p_s,p_t,p} \int_\Omega p_s(x)\,dx \tag{12}$$

subject to the constraints (8), (9), (10) and (11). In this paper, we call (12) the *primal model* and all flow functions p_s, p_t and p *primal variables*.

2.3. Primal-Dual Model

By introducing the multiplier λ, also called the *dual variable*, to the linear equality of flow conservation (11), the continuous maximal flow model (12) can be written as its equivalent *primal-dual model*:

$$\max_{p_s,p_t,p}\min_{\lambda} \int_\Omega p_s\,dx + \int_\Omega \lambda\big(\operatorname{div} p - p_s + p_t\big)\,dx \tag{13}$$
$$\text{s.t.}\quad p_s(x) \le C_s(x)\,,\, p_t(x) \le C_t(x)\,,\, |p(x)| \,\le\, C(x)\,.$$

Rearranging the primal-dual formulation (13) gives

$$\max_{p_s,p_t,p}\min_{\lambda} \int_\Omega \big\{\big(1-\lambda\big)p_s + \lambda p_t + \lambda \operatorname{div} p\big\}\,dx \tag{14}$$
$$\text{s.t.}\quad p_s(x) \,\le\, C_s(x)\,,\, p_t(x) \le C_t(x)\,,\, |p(x)| \,\le\, C(x)\,.$$

2.4. Dual Model: Continuous Min-Cut

Clearly, optimizing the dual variable λ of the primal-dual problem amounts to the primal max-flow model (12). Likewise, optimizing the flow variables p_s, p_t and p of the primal-dual model (14) leads to its equivalent *dual model*:

$$\min_{\lambda(x)\in[0,1]} \int_\Omega \big\{\big(1-\lambda\big)C_s + \lambda C_t\,dx + C\,|\nabla\lambda|\,\big\}\,dx\,. \tag{15}$$

In order to show this, let us first consider the following optimization problem

$$f(q) \,=\, \max_{p\le C} p\cdot q\,. \tag{16}$$

When $q < 0$, p can be chosen to be a negative infinity value in order to maximize the value $p \cdot q$, i.e. $f(q) = +\infty$. Hence, we must have $q \ge 0$ so as to make the function $f(q)$ meaningful and it follows

$$\begin{cases} \text{if } \mathrm{q} = 0\,, & \text{then } \forall p < C \text{ and } f(q) \text{ reaches maximum } 0 \\ \text{if } q > 0\,, & \text{then } p = C \text{ and } f(q) \text{ reaches maximum } q\cdot C \end{cases}.$$

Therefore, the function $f(q)$ can be reformulated by

$$f(q) \,=\, q\cdot C\,, \quad q \ge 0\,. \tag{17}$$

The function $f(q)$ given by (16) provides us a prototype to maximize the source flow $p_s(x)$ and sink flow $p_t(x)$ pointwise in the primal-dual model (14). At each position $x \in \Omega$, in view of (17), we have

$$\begin{aligned} f_s(x) &= \max_{p_s(x) \le C_s(x)} \big(1 - \lambda(x)\big) \cdot p_s(x)\,, \\ \Longrightarrow f_s(x) &= \big(1 - \lambda(x)\big) \cdot C_s(x)\ ,\ 1 - \lambda(x)\ \ge\ 0\,. \end{aligned} \tag{18}$$

and

$$\begin{aligned} f_t(x) &= \max_{p_t(x) \le C_t(x)} \lambda(x) \cdot p_t(x) \\ \Longrightarrow f_t(x) &= \ \lambda(x) \cdot C_t(x)\,, \quad \lambda(x)\ \ge\ 0\,. \end{aligned} \tag{19}$$

For the spatial flow $p(x)$, it is well known [20] that:

$$\max_{|p(x)| \le C(x)} \int_\Omega \lambda \,\mathrm{div}\, p \, dx \ = \ \int_\Omega C\,|\nabla \lambda|\ dx\,. \tag{20}$$

By (18), (19) and (20), it is easy to see that maximizing flows p_s, p_t and p in (14) gives rise to (15).

When $C(x)$ is constant in Ω, e.g. $C(x) = \alpha$, we note that (15) just coincides with the Chan-Esedoglu model (1) proposed in [10]. When $C(x)$ is a so-called edge detector, (15) coincides with the model studied by Bresson et. al. [8]. We focus on the case when $C(x) = \alpha$ and prove the following proposition based on its equivalent max-flow model (12) and primal-dual model (14). The results can be easily extended to its general version (15).

Proposition 1. *Let p_s^*, p_t^*, p^* and $\lambda^*(x)$ be the optimal primal-dual pair of* (13) *when $C(x) = \alpha$. Then each level set function $u^\ell(x)$, $\forall \ell \in (0, 1]$, of $\lambda^*(x)$:*

$$u^\ell(x)\ :=\ \left\{ \begin{array}{ll} 1\,, & \lambda^*(x) > \ell \\ 0\,, & \lambda^*(x) \le \ell \end{array} \right. ,$$

gives a global binary solver of the nonconvex min-cut problem:

$$\min_S \int_{\Omega \setminus S} C_s(x)\, dx \ + \ \int_S C_t(x)\, dx \ + \ \alpha L_S \tag{21}$$

where L_S is the length of the the boundary of S.

Moreover, each cut energy given by the indicator function $u^\ell(x)$ has the same energy as its maximal flow energy:

$$\int_\Omega p_s^*(x)\, dx\,.$$

The proof is given as a supplementary material [1]. The energy of each cut given by $u^\ell(x)$ is equal to its associated max-flow energy by (12). Chan *et al*. [10] also gave a proof of the first part through the coarea formula.

In view of Prop. 1, the variational max-flow problem (12) leads to the segmentation of Ω together with a 'tight boundary', i.e. a minimal cut, by its optimal multiplier λ^*; and vice versa, i.e. the variational max-flow model (12) and its equivalent min-cut model (15) globally solve the nonconvex min-cut problem (21).

2.5. 'Saturated'/'Unsaturated' Flows and Cuts

Now we consider the function $f(q)$ in (16): for the given q and its associated optimal p^*, if $p^* < C$ strictly, by means of variations, its variation directly leads to $q = 0$ as its variation δp can be both negative and positive; on the other hand, if $p^* = C$, its variation over the constraint is $\delta p < 0$ which gives $q > 0$. It follows that if $p^* < C$, i.e. 'unsaturated', then $q = 0$ which leads to the so-called 'cut' in the sense of graph cut.

In the same manner, through (9), it is easy to see that when the optimal source flow $p_s^*(x) < C_s(x)$ at $x \in \Omega$, i.e. 'unsaturated', we must have $1 - \lambda(x) = 0$ at x and $f_s(x) = (1 - \lambda(x))p_s^*(x) = 0$, which means that at the position x the source flow $p_s^*(x)$ has no contribution to the energy function. The flow $p_s^*(x)$, from the source s to x, can be 'cut' off from the energy function of (14). The same holds for the sink flow $p_t^*(x)$: the 'unsaturated' sink flow $p_t^*(x)$ at x gives $\lambda(x) = 0$, which can be cut off. Observe this, only 'saturated' source and sink flows have contributions to the energy.

For the spatial flow fields $p(x)$, let $C_{\mathrm{TV}}^\alpha := \{p \,|\, \|p\|_\infty \le \alpha\,,\, p_n|_{\partial\Omega} = 0\}$. Obviously,

$$\max_{p \in C_{\mathrm{TV}}^\alpha} \langle \mathrm{div}\, p, \lambda \rangle \ = \ \max_{p \in C_{\mathrm{TV}}^\alpha} \langle p, \nabla \lambda \rangle\ . \tag{22}$$

The extremum of the inner product $\langle p, \nabla\lambda\rangle$ in (22) just indicates the normal cone-based condition of $\nabla\lambda$ [12]:

$$\nabla \lambda \ \in \ N_{C_{\mathrm{TV}}^\alpha}(p)\,. \tag{23}$$

Then we simply have:

$$\nabla\lambda(x) \neq 0\,, \qquad \text{if} \quad |p^*(x)| = \alpha\ , \tag{24a}$$

$$\nabla\lambda(x) = 0\,, \qquad \text{if} \quad |p^*(x)| < \alpha \tag{24b}$$

where p^* is the optimal value to maximize (22).

In other words, for some position $x \in \Omega$ where the flow $p^*(x)$ is 'saturated', i.e. $|p^*(x)| = \alpha$, we must have $\nabla\lambda(x) \neq 0$, i.e. there exists jumps of $\lambda(x)$ locally, i.e. a 'cut' locally. For some local area $x \in \Omega$ where the flow variable $p^*(x)$ is not 'saturated', i.e. $|p^*(x)| < \alpha$, we must have $\nabla\lambda(x) = 0$, i.e. $\lambda(x)$ is locally constant.

3. Supervised Max-Flow and Min-Cut

In this section, we study the continuous max-flow and min-cut models with priori given supervision constraints. By simple modifications, we propose new supervised max-flow and min-cut models, which implicitly encode the priori labeled information and share the same complexities with the unsupervised ones.

In contrast to the continuous max-flow and min-cut investigated above, supervised max-flow/min-cut computes

the optimal partition with priori information about some points or areas, e.g. some image pixels have already been labeled, in advance, as foreground or background. Supervised image segmentation can therefore be modeled as the constrained min-cut problem:

$$\min_{S} \int_{S\setminus\Omega_f} C_s(x)\,dx + \int_{(\Omega\setminus\Omega_b)\setminus S} C_t(x)\,dx + \alpha L_S \quad \text{s.t. } \Omega_f \subset S \subset \Omega\setminus\Omega_b\,. \tag{25}$$

where $\Omega_f, \Omega_b \subset \Omega$ are the two disjoint areas pointed out priori: Ω_f belongs to the foreground or objects and Ω_b belongs to the background.

We define two indicator functions:

$$u_f(x) = \begin{cases} 1, & x \in \Omega_f \\ 0, & x \notin \Omega_f \end{cases},\ u_b(x) = \begin{cases} 0, & x \in \Omega_b \\ 1, & x \notin \Omega_b \end{cases} \tag{26}$$

As Ω_f and Ω_b are disjoint, we obviously have

$$u_f(\Omega_b) = 0\,, \quad u_b(\Omega_f) = 1\,. \tag{27}$$

3.1. Primal Model: Supervised Max-Flow

We consider the supervised max-flow model as a problem of flow cost. For the source flow $p_s(x)$: it flows from the source s to each spatial pixel $x \in \Omega$; when $x \in \Omega_b$, the flow is valued as zero as it passes a known background pixel; otherwise, it is valued as the full flow $p_s(x)$. Therefore, in view of $u_b(\Omega_b) = 0$ and $u_b(\Omega\setminus\Omega_b) = 1$ (26), the total cost from the source p_s in Ω is given by $\int_\Omega u_b(x)p_s(x)\,dx$. Concerning the 'total cost' of the sink flow $p_t(x)$: it flows from each spatial pixel x to the sink t; when $x \in \Omega_f$, the sink flow costs $-p_t(x)$ where its negative sign means it reduces the cost; otherwise, the sink flow costs nothing, likewise, in view of $u_f(\Omega_f) = 1$ and $u_f(\Omega\setminus\Omega_f) = 0$ (26), we can evaluate the total cost of p_t in Ω by $-\int_\Omega u_f(x)p_t(x)\,dx$.

Observe the *continuous max-flow* problem (12), we then formulate the *supervised max-flow model* as

$$\max_{p_s,p_t,p} \int_\Omega u_b(x)p_s(x)\,dx - \int_\Omega u_f(x)p_t(x)\,dx \tag{28}$$

subject to the flow constraints (8), (9), (10) and (11). (28) is also called the primal model of the supervised max-flow / min-cut problem.

In the special case when no priori information about foreground and background is given, then we have the two indicator functions $u_f(x) = 0$ and $u_b(x) = 1$, $\forall x \in \Omega$. It can be easily checked that the supervised max-flow problem (28) coincides with the max-flow model (12) in this case.

Introduce the multiplier function λ, as (13), we then have the equivalent primal-dual formulation of (28):

$$\max_{p_s,p_t,p}\min_{\lambda} \int_\Omega u_b(x)p_s(x)\,dx - \int_\Omega u_f(x)p_t(x)\,dx + \int_\Omega \lambda(x)\big(\operatorname{div} p(x) - p_s(x) + p_t(x)\big)\,dx \quad \text{s.t. } p_s(x) \le C_s(x)\,,\ p_t(x) \le C_t(x)\,,\ |p(x)| \le C(x)\,, \tag{29}$$

which can be equally rearranged as

$$\max_{p_s,p_t,p}\min_{\lambda} \int_\Omega (u_b - \lambda)p_s\,dx + \int_\Omega (\lambda - u_f)p_t\,dx + \int_\Omega \lambda(x)\operatorname{div} p(x)\,dx \quad \text{s.t. } p_s(x) \le C_s(x)\,,\ p_t(x) \le C_t(x)\,,\ |p(x)| \le C(x)\,. \tag{30}$$

3.2. Dual Model: Supervised Min-Cut

The maximization of (30) over all flows p_s, p_t and p, subject to (18), (19) and (20), leads to the *supervised min-cut model*, which is the equivalent dual model to (28):

$$\min_{\lambda} \int_\Omega \big(u_b - \lambda\big)C_s\,dx + \int_\Omega \big(\lambda - u_f\big)C_t\,dx + \int_\Omega C(x)\,|\nabla\lambda(x)|\,dx \quad \text{s.t. } u_f(x) \le \lambda(x) \le u_b(x)\,. \tag{31}$$

In this paper, we focus on $C(x) = \alpha$, $\forall x \in \Omega$, then (31) can be equivalently written as

$$\min_{\lambda} \int_\Omega \big(u_b - \lambda\big)C_s\,dx + \int_\Omega \big(\lambda - u_f\big)C_t\,dx + \alpha\int_\Omega |\nabla\lambda(x)|\,dx \quad \text{s.t. } u_f(x) \le \lambda(x) \le u_b(x)\,. \tag{32}$$

Since $u_b(x)$ and $u_f(x)$ are given priori, (32) can be shortened as:

$$\min_{\lambda} \int_\Omega \lambda\big(C_t - C_s\big)\,dx + \alpha\int_\Omega |\nabla\lambda(x)|\,dx \quad \text{s.t. } u_f(x) \le \lambda(x) \le u_b(x)\,. \tag{33}$$

Consider (32) and (33), it is easy to verify that the inequality constraint of $\lambda(x)$, by (26) and (27), exactly gives

$$\lambda(\Omega_f) = 1\,, \quad \lambda(\Omega_b) = 0\,. \tag{34}$$

This coincides with the priori information that Ω_f is already labeled as foreground, i.e. $\lambda(\Omega_f) = 1$, and Ω_b is labeled as background, i.e. $\lambda(\Omega_b) = 0$.

In the special case when no priori information about foreground and background is provided, i.e. $u_f(x) = 0$ and

$u_b(x) = 1$ for $\forall x \in \Omega$, the supervised min-cut problem (32) is equivalent to the continuous min-cut problem obviously.

Moreover, we prove that the supervised cut of (25) can also be obtained by thresholding the global optimum λ^* to (32) or (33) in the same manner as Prop. 1.

Proposition 2. *Let p_s^*, p_t^*, p^* and $\lambda^*(x)$ be an optimal primal-dual pair of* (29) *with $C(x) = \alpha$. Then each indicator function $u^\ell(x)$ by rounding $\lambda^*(x)$ where $\ell \in (0, 1]$:*

$$u^\ell(x) := \begin{cases} 1\,, & \lambda^*(x) \geq \ell \\ 0\,, & \lambda^*(x) < \ell \end{cases},$$

is a global solution to the nonconvex supervised min-cut problem (25)*.*

Moreover, each supervised cut given by $u^\ell(x)$ has the same energy as the optimal supervised max-flow energy, i.e.

$$\int_\Omega u_b(x) p_s^*(x)\, dx \;-\; \int_\Omega u_f(x) p_t^*(x)\, dx\,.$$

The proof of Prop. 2 is similar to the proof of Prop. 1 and is given as a supplementary material [1].

4. Algorithms

4.1. Multiplier-Based Max-Flow Algorithm

In this section, we consider an algorithm based on the max-flow formulation (12). The energy function of (13) is just the lagrangian function of (12). To this end, we define its respective augmented lagrangian function as

$$\begin{aligned} L_c(p_s, p_t, p, \lambda) := & \int_\Omega p_s\, dx + \int_\Omega \lambda\big(\operatorname{div} p - p_s + p_t\big)\, dx \\ & - \frac{c}{2} \left\|\operatorname{div} p - p_s + p_t\right\|^2 , \end{aligned} \tag{35}$$

where $c > 0$.

Therefore, we build up the algorithm, see Alg. 1, for the continuous max-flow problem (12) based on the augmented lagrangian method [5]. λ is updated as the multiplier at each iteration.

4.2. Multiplier-Based Supervised Max-Flow Algorithm

Likewise, we consider the algorithm for the supervised max-flow problem (28). Its equivalent primal-dual formulation of (29) is the lagrangian function of (28). Then, we can define its respective augmented lagrangian function as

$$\begin{aligned} L_c(p_s, p_t, p, \lambda) = & \int_\Omega u_b p_s\, dx - \int_\Omega u_f p_t\, dx \\ & + \int_\Omega \lambda\big(\operatorname{div} p - p_s + p_t\big)\, dx \\ & - \frac{c}{2} \left\|\operatorname{div} p - p_s + p_t\right\|^2 . \end{aligned} \tag{36}$$

We propose the multiplier-based supervised max-flow algorithm as in Alg. 2.

Algorithm 1 Multiplier-Based Maximal-Flow Algorithm

Set the starting values p_s^1, p_t^1, p^1 and λ^1, let $k = 1$ and start $k-$th iteration, which includes the following steps, till convergence:

- Optimizing p by fixing other variables

$$\begin{aligned} p^{k+1} &:= \arg \max_{\|p\|_\infty \leq \alpha} L_c(p_s^k, p_t^k, p, \lambda^k)\,. \\ &= \arg \max_{\|p\|_\infty \leq \alpha} -\frac{c}{2} \left\|\operatorname{div} p(x) - F^k\right\|^2 , \end{aligned}$$

  where F^k is a fixed variable. The above formulation gives a projection problem, which can be easily implemented by Chambolle's approach [9];

- Optimizing p_s by fixing other variables

$$\begin{aligned} p_s^{k+1} &:= \arg \max_{p_s(x) \leq C_s(x)} L_c(p_s, p_t^k, p^{k+1}, \lambda^k) \\ &:= \arg \max_{p_s(x) \leq C_s(x)} \int_\Omega p_s\, dx - \frac{c}{2} \left\|p_s - G^k\right\|^2 \end{aligned}$$

  where G^k is a fixed variable and optimizing p_s can be easily computed at each $x \in \Omega$ pointwise;

- Optimizing p_t by fixing other variables

$$\begin{aligned} p_t^{k+1} &:= \arg \max_{p_t(x) \leq C_t(x)} L_c(p_s^{k+1}, p_t, p^{k+1}, \lambda^k) \\ &:= \arg \max_{p_t(x) \in C_t(x)} -\frac{c}{2} \left\|p_t - H^k\right\|^2 , \end{aligned}$$

  where H^k is a fixed variable and optimizing p_t can be simply solved by

$$p_t(x) \;=\; \min(H^k(x), C_t(x))\,;$$

- Update λ by

$$\lambda^{k+1} \;=\; \lambda^k - c\,(\operatorname{div} p^{k+1} - p_s^{k+1} + p_t^{k+1})\,;$$

- Let $k = k+1$ return to the $k+1$ iteration till converge.

5. Experiments

In this work, we show two applications of the proposed max-flow / min cut models: unsupervised image segmentation and supervised image segementation.

5.1. Unsupervised Image Segmentation

For segmenting images unsupervised, two grayvalues f_1 and f_2 are chosen priori for clues to build data terms:

$$C_s(x) \;=\; D(f(x) - f_1(x))\,, \quad C_t(x) \;=\; D(f(x) - f_2(x))\,,$$

Algorithm 2 Multiplier-Based Supervised Max-Flow

Set the starting values p_s^1, p_t^1, p^1 and λ^1, let $k = 1$ and start $k-$th iteration, which includes the following steps, till convergence:

- Optimizing p by fixing other variables

$$\begin{aligned} p^{k+1} &:= \arg \max_{\|p\|_\infty \le \alpha} L_c(p_s^k, p_t^k, p, \lambda^k) \\ &:= \arg \max_{\|p\|_\infty \le \alpha} -\frac{c}{2} \left\| \operatorname{div} p - F^k \right\|^2 ; \end{aligned}$$

  where F^k is some fixed variable and results in a projection approach;

- Optimizing p_s by fixing other variables

$$\begin{aligned} p_s^{k+1} &:= \arg \max_{p_s(x) \le C_s(x)} L_c(p_s, p_t^k, p^{k+1}, \lambda^k) \\ &:= \arg \max_{p_s(x) \le C_s(x)} \int_\Omega u_b p_s \, dx - \frac{c}{2} \left\| p_s - G^k \right\|^2 , \end{aligned}$$

  where G^k is a fixed variable and optimizing p_s can be easily computed at each $x \in \Omega$ pointwise;

- Optimizing p_t by fixing other variables

$$\begin{aligned} p_t^{k+1} &:= \arg \max_{p_t(x) \le C_t(x)} L_c(p_s^{k+1}, p_t, p^{k+1}, \lambda^k) \\ &:= \arg \max_{p_t(x) \in C_t(x)} -\int_\Omega u_f p_t \, dx - \frac{c}{2} \left\| p_t - H^k \right\|^2 , \end{aligned}$$

  where H^k is a fixed variable and optimizing p_t can be also simply solved pointwise;

- Update λ by

$$\lambda^{k+1} = \lambda^k - c \left(\operatorname{div} p^{k+1} - p_s^{k+1} + p_t^{k+1} \right) ;$$

- Let $k = k+1$ return to the $k+1$ iteration till converge.

where $D(\cdot)$ is some penalty function. Here denoising binary images (see 1st row of Fig. 1) is regarded as a segmentation problem.

Fig. 1 shows two experiment results of unsupervised max-flow model obtained by Alg. 1. By the computed λ^* given at the second graph of each row, we see $\lambda^*(x)$ is binary nearly everywhere of Ω. Segmentation is obtained by simply thresholding λ^*. In contrast to PDE decent methods [10], the proposed algorithm often converges within 100 iterations and reliable for a wide range of c.

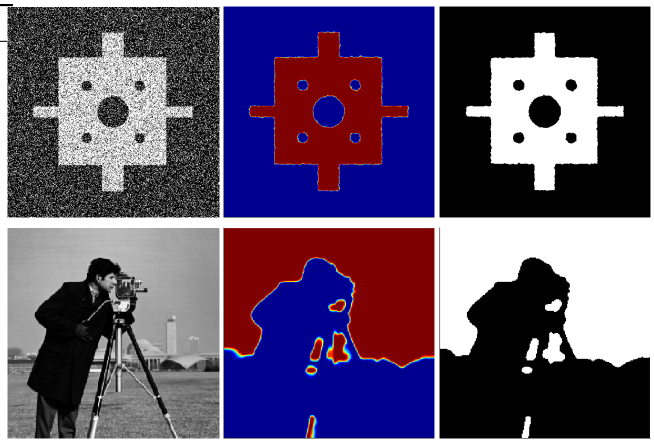

Figure 1. **1st row** shows an experiment of denoising a binary image. **2nd row** gives the result of image segementaion by gray values. **Left column:** The original images f. **Middle column:** The obtained optimum of λ^* respectively. **Right column:** The segmentation achieved by thresholding λ^* with some $\ell \in (0, 1)$ as proposed in Prop. 1.

5.2. Supervised Image Segmentation

For supervised image segmentation, the Middlebury data set [21] is used, see images in Fig. 2, as examples. The corresponding data terms, i.e. $C_s(x)$ and $C_t(x)$, are based on Gaussian mixture color models of foreground and background and provided in advance. It is not required for us to put a very large values to data in the marked areas Ω_f and Ω_b as proposed in (28). In the experiments, we simply put data to be zero at Ω_f and Ω_b, in contrast to graph-based supervised image segmentation.

As a comparison, the tree-reweighted message passing method [22, 14] and α expansion method [7, 6] are applied. It is easy to see that there is no visual artifact in our results, the metrication errors are avoided

6. Conclusions and Future Topics

We study the continuous max-flow and min-cut models, with or without supervised constraints, in this paper. The dualities between max-flow and min-cut are constructed by variational analysis. In this regard, conceptions applied in graph cuts can be explained under a variational perspective and new theoretical results are derived in a natural way. The proposed multiplier-based max-flow algorithms provide reliable numerical schemes. In contrast to discrete graph-based methods, the algorithms can be speeded up by a multigrid and parallel implementation.

References

[1] Supplementary material.

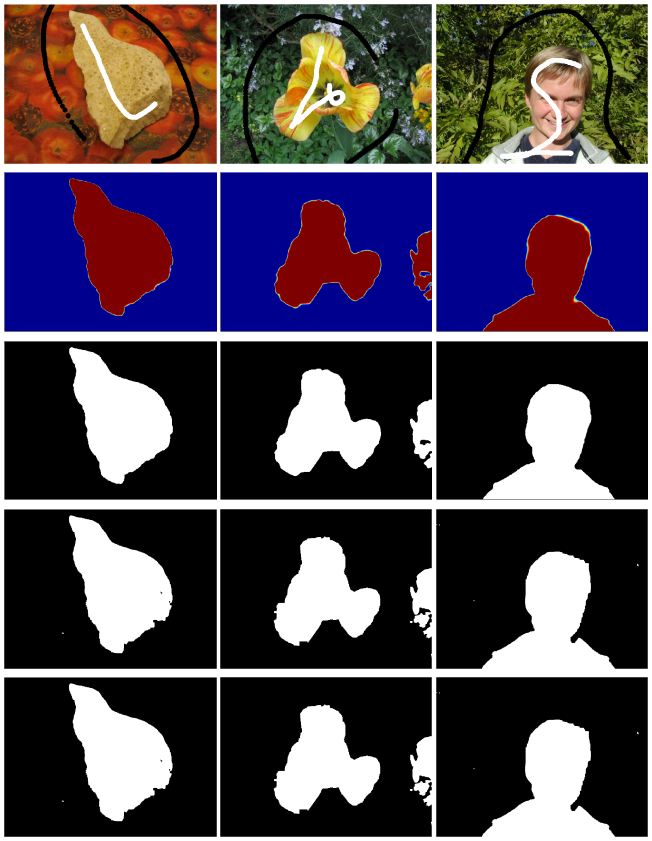

Figure 2. **1st. row:** The three given images, from the Middlebury data set, with pixels marked as foreground (white) and background (black). **2nd row:** computation result of λ^* to each image shown by color images, 0: blue and 1: red. **3rd row:** the black-white segmentation result by a threshold of λ^*. **4th and 5th rows:** respective results computed from tree-reweighted message passing method [22, 14] and α expansion algorithm [7, 6].

[2] B. Appleton and H. Talbot. Globally optimal surfaces by continuous maximal flows. In *Digital Image Computing: Techniques and Applications*, pages 987–996, 2003.

[3] B. Appleton and H. Talbot. Globally minimal surfaces by continuous maximal flows. *IEEE PAMI*, 28:2006, 2006.

[4] E. Bae, J. Yuan, and X. Tai. Convex relaxation for multipartitioning problems using a dual approach. Technical report CAM09-75, UCLA, CAM, September 2009.

[5] D. P. Bertsekas. *Nonlinear Programming*. Athena Scientific, September 1999.

[6] Y. Boykov and V. Kolmogorov. An experimental comparison of min-cut/max-flow algorithms for energy minimization in vision. *IEEE PAMI*, 26:359–374, 2001.

[7] Y. Boykov, O. Veksler, and R. Zabih. Fast approximate energy minimization via graph cuts. *IEEE PAMI*, 23:2001, 2001.

[8] X. Bresson, S. Esedoglu, P. Vandergheynst, J.-P. Thiran, and S. Osher. Fast global minimization of the active contour/snake model. *Journal of Mathematical Imaging and Vision*, 28(2):151–167, 2007.

[9] A. Chambolle. An algorithm for total variation minimization and applications. *Journal of Mathematical Imaging and Vision*, 20(1-2):89–97, 2004.

[10] T. Chan, S. Esedoḡlu, and M. Nikolova. Algorithms for finding global minimizers of image segmentation and denoising models. *SIAM J. Appl. Math.*, 66(5):1632–1648 (electronic), 2006.

[11] D. M. Greig, B. T. Porteous, and A. H. Seheult. Exact maximum a posteriori estimation for binary images. *Journal of the Royal Statistical Society, Series B*, pages 271–279, 1989.

[12] J.-B. Hiriart-Urruty and C. Lemaréchal. *Convex analysis and minimization algorithms. I*, volume 305 of *Fundamental Principles of Mathematical Sciences*. Springer-Verlag, Berlin, 1993. Fundamentals.

[13] V. Kolmogorov. What metrics can be approximated by geocuts, or global optimization of length/area and flux. In *ICCV*, pages 564–571, 2005.

[14] V. Kolmogorov. Convergent tree-reweighted message passing for energy minimization. *IEEE PAMI*, 28(10):1568–1583, 2006.

[15] V. Kolmogorov and R. Zabih. What energy functions can be minimized via graph cuts. *IEEE PAMI*, 26:65–81, 2004.

[16] J. Lellmann, J. Kappes, J. Yuan, F. Becker, and C. Schnörr. Convex multi-class image labeling by simplex-constrained total variation. Technical report, HCI, IWR, Uni. Heidelberg, November 2008.

[17] V. Lempitsky and Y. Boykov. Global optimization for shape fitting. In *In CVPR*, 2007.

[18] T. Pock, A. Chambolle, H. Bischof, and D. Cremers. A convex relaxation approach for computing minimal partitions. In *In CVPR*, Miami, Florida, 2009.

[19] G. Strang. Maximal flow through a domain. *Mathematical Programming*, 26:123–143, 1983.

[20] G. Strang. Maximum flows and minimum cuts in the plane. *Advances in Mechanics and Mathematics*, III:1–11, 2008.

[21] R. Szeliski, R. Zabih, D. Scharstein, O. Veksler, A. Agarwala, and C. Rother. A comparative study of energy minimization methods for markov random fields. In *ECCV*, pages 16–29, 2006.

[22] M. Wainwright, T. Jaakkola, and A. Willsky. Map estimation via agreement on (hyper)trees: Message-passing and linear programming approaches. *IEEE Transactions on Information Theory*, 51:3697–3717, 2002.